Thesis for the degree of Master of Science

이학석사학위논문

Statistical Analysis of electric properties of octanemonothiols and octanedithiols PEDOT:PSS Junctions devices : comparison between the methyl end group and the thiol end group

Octanemonothiol과 Octanedithiol PEDOT:PSS 접합 소자의 전기적 특성에 관한 통계적 분석: 메틸 말단기와 싸이올 말단기간의 비교를 통하여

Hanki Lee

Department of Physics and Astronomy

Seoul National University

서울대학교 대학원

물리천문학부

이 한 기

2014

Abstract

In this study, a large number of octanemonothiol (C8) and octanedithol (DC8) molecular electronic devices with PEDOT:PSS (3,4-ethylenedioxythiophene) interlayer were fabricated and statistical analysis were performed to the electronic properties of these devices. From the analysis, several statistical values such as arithmetic mean, median, Gaussian mean, arithmetic standard deviation, adjusted absolute median deviation, and Gaussian standard deviation were obtained by corresponding methods and also Gaussian plot of histograms of Log_{10}(current density (J)) was fitted by Gaussian methods. Continually the current density–voltage (J-V) characteristics from the statistically representative data for C8 and DC8 devices were investigated and it was, from the investigation, found that the conductivity of C8 is higher than that of DC8 by a factor of ~10. Owing to difference properties of PEDOT and PSS, it can be implied that the C8 with methyl end groups would contact with the PEDOT and DC8 with thiol end groups would contact with the PSS. Finally it is conclusion that the difference of the conductivity of C8 and DC8 with PEDOT:PSS junction devices is originated from the difference of the contact properties between the C8 and DC8 with PEDOT:PSS-interlayer molecular junctions.

Contents

List of Figures

List of Tables

1. Introduction

1.1 Introduction

In 1960, Herwald and Angello stated that 'The trend in electronics circuit construction is toward microminiaturization and molecular electronics.' in their article in 'Science'.[1] In this article, they also supposed that 'the boundaries between materials and devices and between devices and circuits are being removed, and we shall see an integration of disciplines in the future development of molecular electronics.' After 14 years from the prediction, Aviram and Ratner first proposed a method of making a rectifier based on a single organic molecule in 1974.[2] Since the electric properties of molecules can be easily changed by molecular structure and synthesis, molecular electronic devices, in theory, has unlimited possibilities for technological development.[3] Self-assembled monolayer (SAM) is common method in the molecular device fabrication and also popular subject in the field of molecular electronic. In particular SAM of alkanethiol (HS or CH_3-$(CH_2)_n$-SH) ,as were used by Mann and Kuhn[4], are a perfect benchmark for any new experimental testbed in molecular electronics.[3] Because alkanthiols possess a large energy gap between the highest occupied molecular orbital(HOMO) and lowest unoccupied molecular orbital(LUMO) of about 8-10 EV [5,6], these molecules are insulating and, consequently, a tunneling current is expected which decreases exponential with increasing molecule length.[3]

The fabrication of molecular electronic junction using a conductive polymer (PEDOT:PSS; 3,4-ethylenedioxythiophene) between the top electrode and the molecules has been one of the most successful techniques in terms of high device yields and stable junctions. The use of a conducting polymer as a top electrode on top of a SAM in an insulating photoresist matrix

has proven to result in a device with a stability of at least several months in air, no degradation upon sweeping, and working devices with diameters up to 100 μm. Furthermore, the yield of working devices is close to 100% and the technology is compatible with standard integrated circuit fabrication processes.[7] Nevertheless, the use of a conductive polymer presents some uncertainties as a platform for molecular devices because the properties of the interface between the polymer layer and the molecules are not thoroughly understood.[3,7-11] Thus understanding properties of the interface between the polymer layer and the molecules has been crucial demanding task in the field of molecular electronics.

In this study, sufficient number of octanemonothiol (C8; 112 devices) and octanedithol (DC8; 128 devices) molecular devices with PEDOT:PSS interlayer were fabricated for a meaningful statistical analysis which will give an insight to understating properties of the interface. To begin with, the electrical properties of the fabricated molecular devices, current density data from -1V to 1V, were measured and histograms of Log_{10}|current density (J)| was made from them. Several statistical estimates; arithmetic mean (μ_A), median (μ_M), Gaussian mean (μ_G), arithmetic standard deviation (σ_A), adjusted absolute median deviation (σ_M), and Gaussian standard deviation (σ_G) could be obtained and analyzed statistically. Next the conductivity of C8 devices and the conductivity of DC8 devices were studied once more by comparing their current density-voltage (J-V) characteristics from representative data. Also, refer to the characteristics of PEDOT and PSS studied in proceeding research, the relation between octanethiol's end groups (Methyl and Thiol) with the PEDOT:PSS was suggested to understand the interface properties. Finally the relation between the conductivity and the contact properties in molecule-PEDOT:PSS interface was discussed to understand the difference in the electrical characteristics

1.2 Conduction mechanism through Molecular Junctions

In a molecular junction, the Fermi level alignment is critical in determining the conduction mechanism.[12] Created by the overlap of the atomic orbitals of a molecule's constituents, two molecular orbitals, lowest unoccupied molecular orbital (LUMO) and highest occupied molecular orbital (HOMO), play similar role as a conduction band and valence band in a semiconductor, respectively. The Fermi level of the metallic contacts generally does not align with either the HOMO or the LUMO of the molecule, but instead lies close to the center of the gap.[13] This energy level mismatch gives rise to a contact barrier, including a height and a thickness of this barrier and the presence of defects.[14]

There are various models to explain conduction mechanism which have their characteristic behavior, temperature dependence, and voltage dependence; 1) Direct Tunneling 2) Fowler-Nordheim Tunneling 3) Thermionic Emission and 4) Hopping conduction. Here we focus on direct tunneling as main conduction mechanism in molecular electric devices made with short length (< 1-2 nm) of molecules. Figure 1 is an energy band diagram describing the quantum mechanical tunneling through a thin gap. In this diagram, positive voltage is applied to the right side electrode, thus the Fermi energy of the right electrode is lowered with respect to the left side. The potential barrier Φ_B is formed by the gap (molecule in this case) between the left and right side electrodes. When an electron from occupied states on the left side tunnels into empty states on the right side, one can consider two types of direct tunneling; elastic tunneling and inelastic tunneling. In the elastic tunneling, the energy of the tunneling electron from left to right side is conserved whereas that is not conserved in the inelastic tunneling. In the inelastic tunneling, the lost energy from the tunneling electron transfers to molecular vibrational modes. This electron-vibration mode coupling occurs at characteristic frequency ω of molecular vibration modes.[15,16] Only elastic tunneling is considered for simple

discussion in this study.

Coherent and incoherent tunneling have been two distinct transport mechanism which were extensively discussed in the literature.[17,18] I-V characteristics as a function of temperature and molecular length are essential to identify the conduction mechanism; Coherent tunneling is typified by a temperature independent. On the contrary, incoherent tunneling is characterized by a weak length dependent. Coherent tunneling dominates in short molecules. In the contrast, incoherent tunneling occurs along long-conjugated molecular wires. Following equations represent the character of coherent tunneling. According to this equation, the conductance value (G) decreases exponentially as the molecular length increases.

$$G \propto \exp(-\beta d) \qquad (1)$$

Here, d is the molecular length and β is the tunneling decay coefficient.

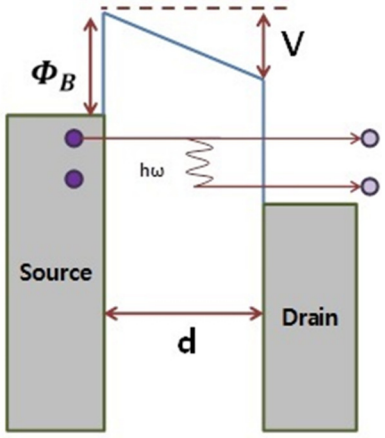

Figure 1. A schematic Energy band diagram of a molecular junction

1.3. The molecule-electrode interface

The interface between the molecules and the electrodes can be divided into chemisorbed or physisorbed contact.[19] Not fully understood yet, the formation of Au–S bond has known to be a chemisorbed contact.[19~22] The difference between a chemisorbed contact and a physical contact can lead to a change of a few orders of magnitude in conductivity of the junction.[23-25] In the case of alkanethiol molecules, this difference in conductivity between physisorbed and chemisorbed contacts can be understood by describing current through the molecular junction with the Landauer formula [25-31], stating that the conductance G is given by:

$$\mathrm{G} = \frac{2e^2}{h} \times T_b \times T_{mol} \times T_t \qquad (2)$$

where e is the elementary charge, h is the Planck's constant and T_b, T_t and T_{mol} are the transmission coefficients of the bottom interlayer contact, top interlayer contact and the molecule, respectively. From this formula, it can be inferred that a change in transmission of any contacts will alter the absolute value of the conductance with the same factor. Thus, to make a good comparison between the obtained currents per molecule, the differences in transmission of the second contact must be accounted for. One prime example is the contact difference between alkanemonothiols and alkanedithiols.[3] In this study, we compare the contact difference between octanemonothiols and octanedithiols with PEDOT:PSS interlayer.

1.4 Statistical Analysis method

Simmons model [32] is used as an initial point to start our statistical analysis. When the Simmons model holds, current density (J) depends exponentially on molecular contact length (d) as followed;

$$J \propto \exp(-\beta d);\ \text{where } \beta \text{ is the tunneling decay constant.}$$

Thus a normal distribution of d would translate to a normal distribution of Log |J/(A/cm2)|, simply log|J|.[33] Normal distribution is so called Gaussian distribution and defined by following equation;

$$f(x) = \frac{1}{\sigma_G \sqrt{2\pi}} exp\left[\frac{(x-\mu_G)^2}{2{\sigma_G}^2}\right] \qquad (3)$$

where μ_G is the Gaussian mean and σ_G is the Gaussian standard deviation. The accuracy of the Gaussian mean and standard deviation depends heavily whether all informative measurements of log|J| are randomly sampled from a normal distribution.[33]

For more ample statistical analysis, following methods were also performed in this paper.

(1) Arithmetic mean and standard deviation

Arithmetic mean (μ_A) is the sum of a collection of numbers divided by the number of numbers in the collection.[33] Arithmetic standard deviation (σ_A) is the square root of second moment about μ_A.[34]

(2) Median and median absolute deviation

The median (μ_M) is defined [35-37] as the value for which 50% of the sample is greater than or equal to that value, and 50% of the sample is less than or equal to that value. Though median absolute deviation is useful for visualizing sample, it can't be compared directly like σ_G and σ_A. However, for comparison with them, we can use the following adjusted median absolute deviation (σ_M) as demoted; [38]

$$\sigma_M = 1.4826 \times \text{median}(|x - \mu_M|) \qquad (4)$$

The quantity, median ($|x-\mu_M|$), is called the median absolute deviation, and the factor of 1.4826 adjusts this quantity to correct for underestimation of the sample standard deviation.

2. Experiment

2.1 Conducting Polymer: PEDOT:PSS (3,4-ethylenedioxythiophene)

PEDOT:PSS is a polymer mixture of two ionomers; PEDOT and PSS. PEDOT(chemical structure shown in Figure 2) is a derivative of polythiophene and is usually prepared by polymerization of ethylenedioxythiophene (EDOT). Conductive PEDOT can be prepared by electrochemical or chemical polymerization. PEDOT doped with small anions are insoluble in any solvent. When excess PSS (chemical structure shown in Figure 2) is used as the counter anion for the PEDOT by chemical oxidation, however, PEDOT:PSS can be dispersed in water. The PEDOT chains are attached to the PSS chains through the Coulombic interaction. They are stabilized by the excess PSS. In other words, the excess PSS is used to stabilize PEDOT in water; i.e. the hydrophilic PSS chains form micelles with the hydrophobic PEDOT chains inside. Briefly PEDOT:PSS is a blend of an oxidatively doped, cationic, conducting polythiophene derivative (PEDOT) that is electrostatically bound to a PSS polyanion. PEDOT:PSS combines high conductivity and good transparency in the visible region with excellent stability under ambient conditions and can be easily processed from aqueous dispersions by spin coating.[39-42]

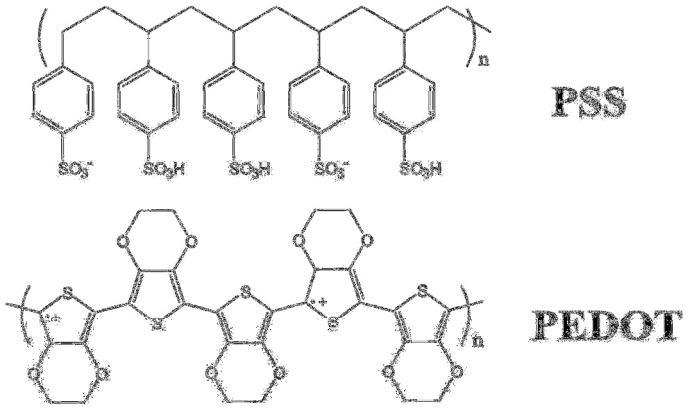

Figure 2. Chemical Structure of PEDOT:PSS [43]

2.2 Self Assembled Monolayer (SAM): Octanemonothiols(C8) and Octanedithiols(DC8)

Octanemonothiol(C8) is a one side's thiol-terminated eight-alkyl chain molecular system ; CH_3-$(CH_2)_8$-SH] and Octanedithiol(DC8) is a both sides thiol-terminated eight-alkyl chain molecular system ; HS-$(CH_2)_8$-SH. As commonly known, self-assembled alkanethiols on Au surface form densely packed and crystalline-like structure with the alkyl chain in an all-trans conformation. [44] The Self Assembled Monolayer (SAM) process is can be explained by following chemical reaction [45,46]

$$R\text{-}SH + Au \rightarrow RS\text{-}Au + o.5\ H_2 \qquad (5)$$

where R is the backbone of the molecule and -SH is a thiol end. This chemical absorption process is indicated to two steps: 1) a swift process that takes minutes (depending on the thiol concentration) and gives ~ 90% of the film thickness 2) a gradual process that lasts hours and reaches the final thickness and contact angle.[44,46] There are three forces suggested to determine this SAM process and the final monolayer structure: the interaction between the thiol head group and gold lattice, dispersion force between alkyl chains (van der Waals force, etc.), and the interaction between the end groups.[47]

Figure 2 shows molecular structures of octanemonothiol (C8) and octanedithiol (DC8) in PEDOT:PSS junction. In the bottom surface, both thiol end groups are chemisorbed with the Au surface in both structures. In the top surface, however, methyl end groups of C8 contact with the PEDOT:PSS junction and thiol end groups of DC8 contact with the PEDOT:PSS junction.

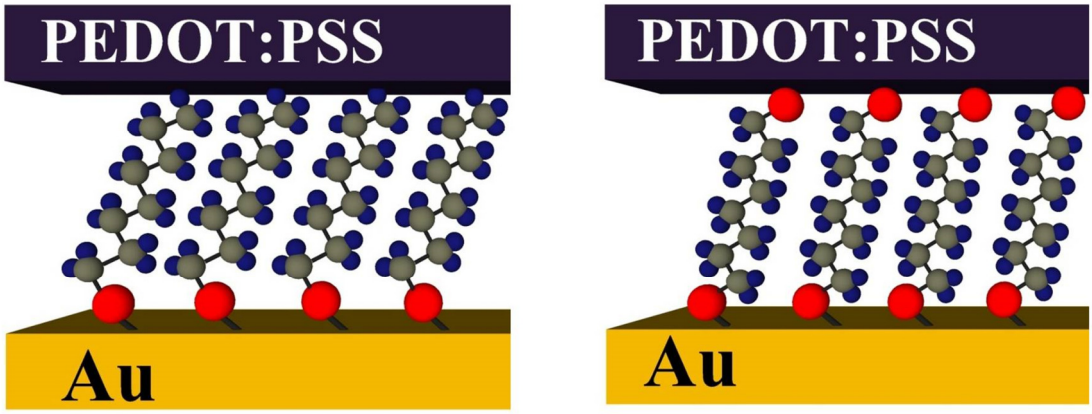

a. Octanemonothiol(C8)

b. Octanedithiol(DC8)

Figure 3. Molecular Structures of C8 and DC8 in PEDOT:PSS Junction

2.3 Device Fabrication

The PEDOT:PSS molecular junction devices (Au-Octanethiol-PEDOT:PSS/Au) fabrication procedures are shown in Figure 3. First, designed Au (500 Å)/Ti (100 Å) bottom electrodes were deposited on a p-type (100) 300 nm thickness SiO_2 substrate using a shadow mask by an electron beam evaporator at a rate of ~0.1 Å/s. Then photoresist (AZ5214) was spin coated on the bottom electrodes to form an insulating wall which electrically isolates the bottom electrodes with the top electrodes. Next the UV photolithography process was performed to make hole structures in the photoresist layer by a mask aligner. The holes were square-shaped and had side lengths ranged from 30 μm to 100 μm with an increment of 10 μm. After the formation of the via-hole pattern, the devices were annealed on a hot plate at ~200 ^{o}C for 2 h 30 min to make the photoresist layer insoluble in ethanol during the formation of the molecular self-assembled monolayer (SAM) on the bottom electrodes. Next the devices were put into 2 mM octanemonothiol (C8) and octanedithiol (DC8) solutions diluted with ethanol to form the SAM on the bottom electrodes for 24hours~48hours. After the SAM process, the devices were rinsed with ethanol to remove residual unbounded molecules. Subsequently PEDOT:PSS was spin coated on the devices for 3 minutes and dried for 3 hours. SAM forming, PEDOT:PSS coating and drying process were all performed in the N^2 gas filled glove box Chamber and at the room temperature. And Au top electrodes (500 Å) were deposited on top of the PEDOT:PSS interlayer using a shadow mask by an electron beam evaporator at a rate of ~0.1 Å/s. To prevent the formation of a direct current path through the PEDOT:PSS layer between the top and bottom Au electrodes, reactive ion etching (RIE) was finally performed with O_2 gas to remove redundant PEDOT:PSS layers on the devices.[48] Figure 4 is the schematic diagram of the device structure of the PEDOT:PSS junction molecular devices. The J-V characteristics of the fabricated devices were measured

by using a semiconductor parameter analyzer (Keithley 4200-SCS) in N^2 gas filled glove box to prevent the degradation by water vapor and O2.

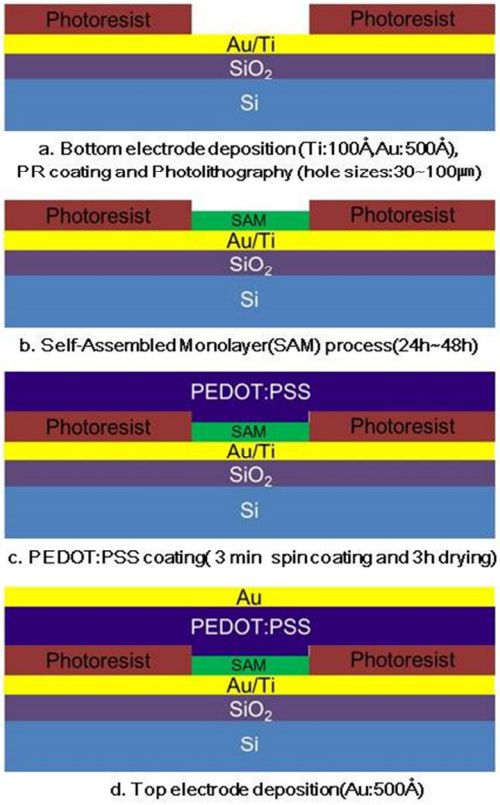

Figure 4. Device Fabrication Procedures of PEDOT:PSS Molecular Junction Devices

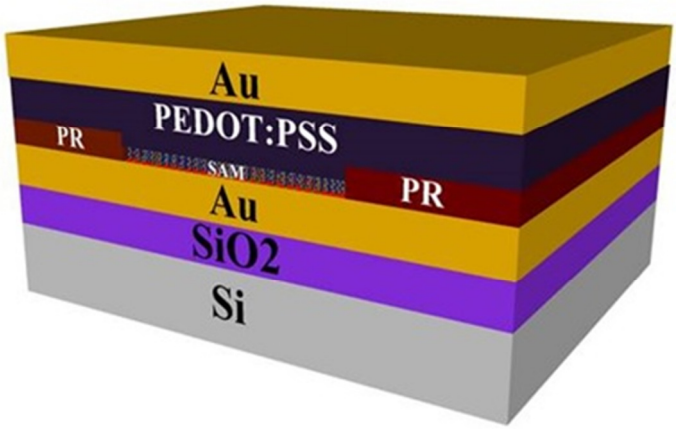

Figure 5. A schematic diagram of the PEDOT:PSS Molecular Junction Device Structure

3. RESULTS AND DISCUSSION

3.1 Statistical analysis of an electric property of C8 and DC8 molecular devices

The statistical approach to molecular electronic devices can provide a useful way to distinguish the transport property of different molecular system.[49] Sufficient number of devices which give trustworthy information are necessary to conduct the statistical analysis. Hence numerous number of device fabrication has been suggested as an initial condition for the analysis in many preceding research. In addition enough yields of 'working' devices are also suggested for the successful analysis. Working devices might be typically defined as a device showing non-linear I-V behavior and not being electrical open and short. Open devices are noisy with a current level normally in pA degree and short devices show Ohmic(linear) I-V characteristics with a current level larger than a few mA.[50]

Accordingly each 112 C8 devices and 128 DC8 devices were fabricated for the statistical analysis in this research. Also, from the above defining criteria, 61 C8 devices and 89 DC8 devices could be selected as working devices. However above mentioned criteria is just basic standard to define informative devices which give valuable data for the statistical analysis. Among the raw working devices, informative devices are still to be distinguished with the non-informative devices by performing certain methodology. There are two major ways to draw a distinction between informative and non-informative data: (1) construct a parametric statistical model [35,36,51] that assumes that informative devices follow a certain probability distribution, while non-informative devices follow a different distribution, or (2) assume that the majority of devices are informative and choose a methodology that is insensitive to

relatively small numbers of extreme data (that is, a "robust" method [38,52]) since these devices are likely to be non-informative.

In this research, the 'informative' working devices were extracted from the devices showing a majority of current densities in the statistical distribution by using a Gaussian distribution function.[53] Precisely 99.7% of the devices from overall population which were included in the interval of the $3\sigma_G$ range between $\mu_G + 3\sigma_G$ and $\mu_G - 3\sigma_G$ were selected as the 'informative' working devices.[49] Figure 5 and 6 show the histograms of $Log_{10}J$ of 'raw' working devices of molecular devices and also their denoted 3 σ_G ranges. First, in figure 5, 61 working C8 devices were in $3\sigma_G$ ranges (99.7% ranges) so selected as the informative. Next, in Figure 6, 89 working DC8 working devices were also in $3\sigma_G$ ranges so selected as same. Outliers (data that lie far from the peak in histograms of $Log_{10}J$) and long tails (larger share of the data to the right of the peak than in a normal distribution) [33] which suggested to be 'non-informative' were excluded by this process. Finally the device yield of 'informative' working devices was each 57/112 = 50.9% for C8 devices and 86/128 = 67.2% for DC8 devices in PEDOT:PSS-electrode molecular junction structure. This yield is significantly larger as compared with the case of metal-molecule-metal junction structure without using PEDOT:PSS interlayer which showed a typical device yield of ~1%.[49] Both histograms were fitted with the Gaussian distribution function (See 1.3 section) and the curves in the figures are the results of this fitting. And figure 7 is the integrated histograms of $Log_{10}J$ of 'informative' working devices of C8 and DC8 molecular. The directed positions in figure 7 by arrows are the Gaussian mean of each distribution and they imply that the $Log_{10}J$ of C8 is slightly larger than that of DC8.

To compare data of C8 and DC8 devices more specifically, statistical methods explained in Section 1.4 were used in this research; 1) Arithmetic 2) Median 3) Gaussian. (Details of each method are explained in Section 1.4.)

Table 1 shows the results from those statistical methods performed to C8 and DC8 PEDOT:PSS junction devices. First the arithmetic mean (μ_A) of C8 and DC8 devices is each 1.24 and 0.77. Next the median (μ_M) of C8 and DC8 devices is each 1.34 and 0.81. And the Gaussian mean (μ_G) of C8 and DC8 devices is each 1.37 and 0.83. As summarized, μ_G of C8 and DC8 molecular devices is found to be larger than μ_A of them by 0.13 and 0.06, respectively. However, μ_G of C8 and DC8 devices is larger than μ_M only by 0.03 and 0.02, respectively. Overall the current density of C8 devices is larger than that of DC8 devices and this fact implies that the conductivity of PEDOT:PSS-C8 molecular devices is higher than that of PEDOT:PSS-DC8 molecular devices. Now compare the standard deviation of each molecular device. First the Arithmetic standard deviation (σ_A) of C8 and DC8 is each 0.56 and 0.66. Next the adjusted absolute median deviation (σ_M) of C8 and DC8 devices is 0.31 and 0.57. And the Gaussian standard deviation (σ_G) of C8 and DC8 devices is each 0.30 and 0.51. In other words, σ_G of C8 and DC8 devices are found to be smaller than σ_A of C8 and DC8 devices by 0.26 and 0.15, respectively. But σ_G of C8 and DC8 devices are smaller than σ_A of C8 and DC8 devices only by 0.01 and 0.06, respectively. Overall the standard deviation of C8 devices is smaller than that of DC8 devices. Because the distributions of $Log_{10}J$ coincide with distribution of molecular contact length from Simmons model [32] and the standard deviation of d is normally proportional to the size of it, the larger standard deviation means the longer molecular length. Therefore the larger standard deviation of DC8 devices implies the longer molecular length of DC8 molecular junction. In other words, the molecular contact length of PEDOT:PSS-DC8 junction might be longer than that of PEDOT:PSS-C8 junction.

From above, we can find that the difference between the arithmetic and Gaussian statistical values of two devices are much larger than that between the median and Gaussian values of them. These results are because μ_A and σ_A respond strongly to long tails (larger share of the

data to the right of the peak than in a normal distribution) and outliers (data that lie far from the peak in histograms of $Log_{10}J$). Since most histograms had long tails and outliers, σ_A was usually found to be greater than σ_G.[33]

For a true normal distribution, it is has been known that any estimates of the standard deviation will tend to be smaller than interquartile range (IQR) which is equal to the difference between the upper and lower quartiles.[54-55] In this research, IQR of C8 and DC8 molecular devices were found to be 0.40 and 0.80, respectively. Comparing them with standard deviation results in Table 1, all standard deviation values of DC8 devices are smaller than its IQR value. Also σ_M and σ_G of C8 devices are smaller than its IQR value. However, due to outliers shown in figure 5, σ_A is not smaller than the IQR value.

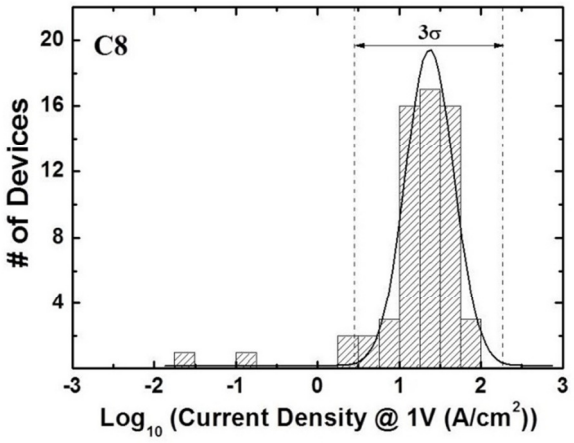

Figure 6. Histogram of logarithmic current devices at 1 V from 'raw' C8 molecular working devices

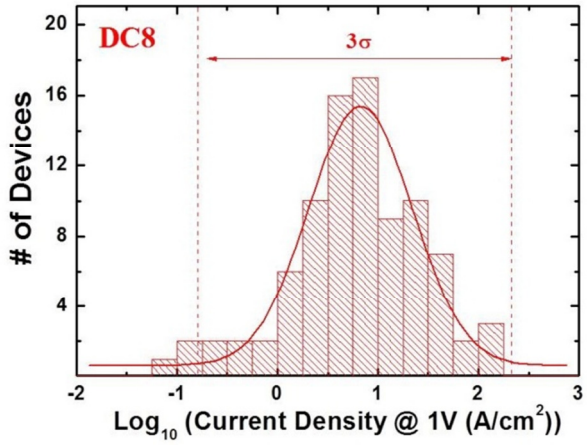

Figure 7. Histogram of logarithmic current devices at 1 V from 'raw' DC8 molecular working devices

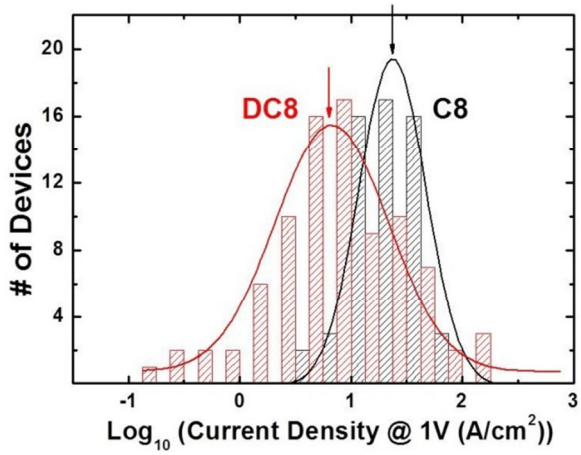

Figure 8. Histogram of logarithmic current densities at 1 V for 'informative' C8 and DC8 working devices.

	μ_A	μ_M	μ_G	σ_A	σ_M	σ_G
C8	1.24	1.34	1.37	0.56	0.31	0.30
DC8	0.77	0.81	0.83	0.66	0.57	0.51

Table1. The list of statistical estimates for C8 and DC8 molecular devices

Note: μ_A: arithmetic mean, μ_M: median, μ_G: Gaussian mean, σ_A: arithmetic standard deviation, σ_M: adjusted absolute median deviation, σ_G: Gaussian standard deviation. The unit of μ_A, μ_M and μ_G is $Log_{10}(A/cm^2)$.

3.2 The electric properties from different contact interface between C8 and DC8 with PEDOT:PSS junctions

Current density reflects the conductivity of different molecular systems.[49] Here the data near from the median of Log_{10} J (see Table 1)were collected as statistical representatives and plotted to current density-Voltage(J-V) characteristics. Figure 8 shows J-V characteristic of C8 and DC8 molecular devices. The plot of C8 devices is clearly distinguished from the plot of DC8 devices. Numerically the J of C8 representative junction is higher than that of DC8 representative junction by a factor of ~10 in the A/cm^2 unit.

These different conductivities of C8 and DC8 representative devices are related to their different contact interfaces with PEDOT:PSS electrodes. As mentioned in Section 1.3, the electrode-molecule interface can be divided into a chemisorbed or physisorbed contact. In this Au-Molecule-PEDOT:PSS junction, the interface of DC8 SAM on the bottom Au (111) has the same ordering structure (tilt angle and packing density) as the C8 SAM on Au(111) .[56] Because the head thiol group of C8 and DC8 will make identical chemisorbed contact with the bottom Au electrode in the same chemical reaction explained in Section 2.2. But the interface of DC8 SAM with the top PEDOT:PSS is different to the interface of C8 SAM with the PEDOT:PSS. Since the thiol end-group of DC8 (-S) contact with the PEDOT:PSS electrode while methyl end-group of C8 ($-CH_3$) contact with the PEDOT:PSS electrode. Thus possible reason of their different conductivities can be originated from their different interface between C8 and DC8 with the PEDOT:PSS junctions. To investigate above assumption more precisely, the research on spin coated PEDOT:PSS has to be studied.

Figure 9 and 10 show the topographic scanning tunneling microscopy (STM) image and cross-sectional (atomic force microscopy) AFM phase image of PEDOT:PSS film. First, Figure 9 shows that PEDOT:PSS films indeed have a granular morphology, with a typical

grain size of about 20~25nm. These grains are also suggested to have the shape of pancake-like structure. Next Figure 10 can be interpreted as side view of PEDOT-rich "pancakes" (dark features) with a thickness of a few nanometers and a diameter of a few tens of nanometers separated by PSS lamellas (bright features). In the normal direction, the separating barriers, that is, the PSS lamellas are quasi-continuous, whereas the separations in the lateral direction do not seem to be fully closed. Clearly, a top view of these lasagna-like structures should look like Figure 9. These STM and X-AFM measurements can be combined into the schematic morphological model as shown in Figure 11. Figre 11 shows that PEDOT-rich clusters (dark) are separated by lamellas of PSS (light) and pancake-like particles as pictured by the dotted lines. Also PEDOT-rich core has a much higher intrinsic conductivity than the PEDOT-depleted grain boundary, which is essentially insulating because PSS is a weak ionic conductor. In other words, due to the fact that PEDOT is a high conductor whereas PSS is a weak one, the current is more easily transported through the PEDOT-rich area than PSS lamellas.[42] Therefore, in the PEDOT:PSS molecular junction, it can be suggested that the conductivity of the junction will be higher when molecules make contact with PEDOT-rich area rather than PSS.

In the Au -C8/DC8-PEDOT:PSS junction, C8 and DC8 make contacts with the bottom electrodes with thiol end group (-S), but the other end of C8 and DC8 which are coated with PEDOT:PSS makes different contacts due to the end group of each type of molecules; i.e. C8 has hydrophobic methyl ($-CH_3$) as the end group whereas DC8 has hydrophilic thiol (-S) as the end group. Though PEDOT:PSS is water-soluble and hydrophilic, PEDOT is itself hydrophobic and PSS is hydrophilic as mentioned in Section 2.1. From this reason, it can be inferred that the hydrophobic methyl end group of C8 would prefer to make contact with hydrophobic PEDOT area than hydrophilic PSS lamellas. Whereas, compared to the C8 case, the hydrophilic thiol end group of DC8 would contact more easily with hydrophilic PSS

lamellas than hydrophobic PEDOT region. Because both thiol and methyl makes physisorbed contact with PEDOT:PSS and , in this case , hydrophobic materials adjoin easily with same nature materials while hydrophilic one do in the same manner. Thus these different contact (methyl-PEDOT and thiol-PSS) properties can explain why the conductivity of C8 devices is higher than that of DC8 devices. Figure 12 shows the schematic representations of C8 with hydrophobic methyl contact to high conducting PEDOT part and DC8 with hydrophilic thiol contact to weak conducting PSS part. Refer to the Landauer model shown in Sec 1.3, the change in the transmission coefficient of top interlayer contact (Here Methyl-PEDOT:PSS and Thiol-PEDOT:PSS) makes different conductivity between the C8 and DC8 devices.

To conclude, PEDOT:PSS-C8 junctions show higher conductivity than PEDOT:PSS-DC8 junctions in that C8 having hydrophobic methyl end groups would smoothly connect to high conducting and hydrophobic PEDOT regions while DC8 which has hydrophilic thiol end groups would smoothly contact with weak conducting and hydrophilic PSS lamellas.

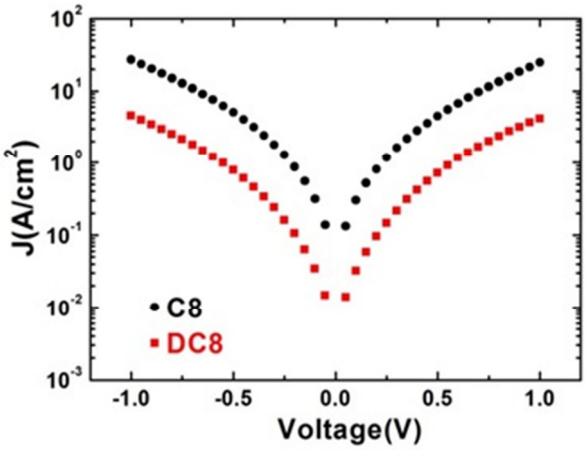

Figure 9. Current density-Voltage (J-V) characteristics of representative C8 and DC8 PEDOT:PSS junction devices

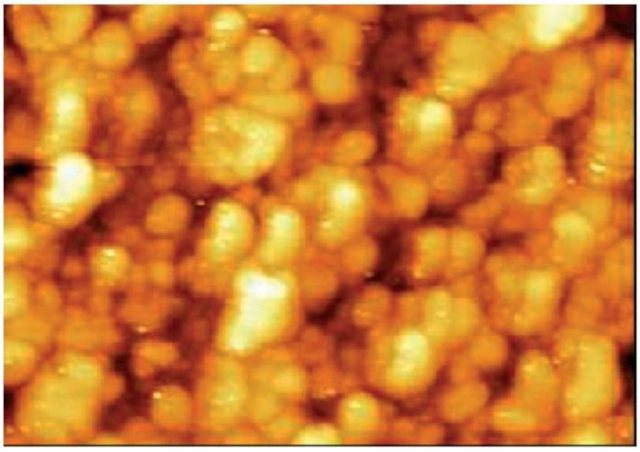

Figure 10. The topographic STM image of PEDOT:PSS on indium tin oxide(ITO) at 2.3V, tunneling current 10pA [41]

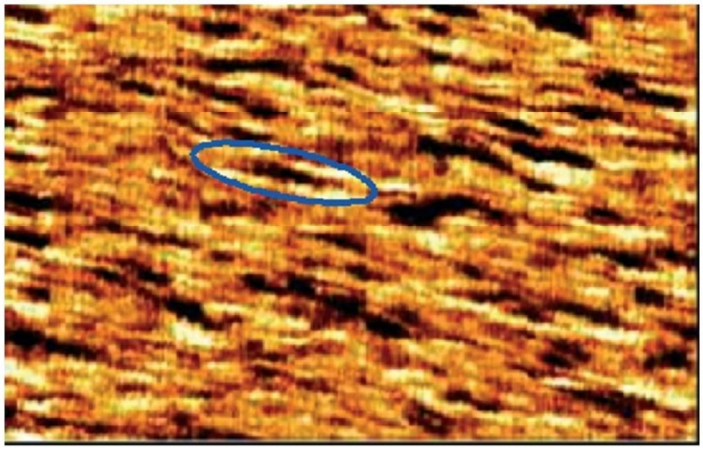

Figure 11. The cross-sectional AFM phase image of cleaved PEDOT:PSS on glass. A pancake like particle is highlighted by the ellipse [41]

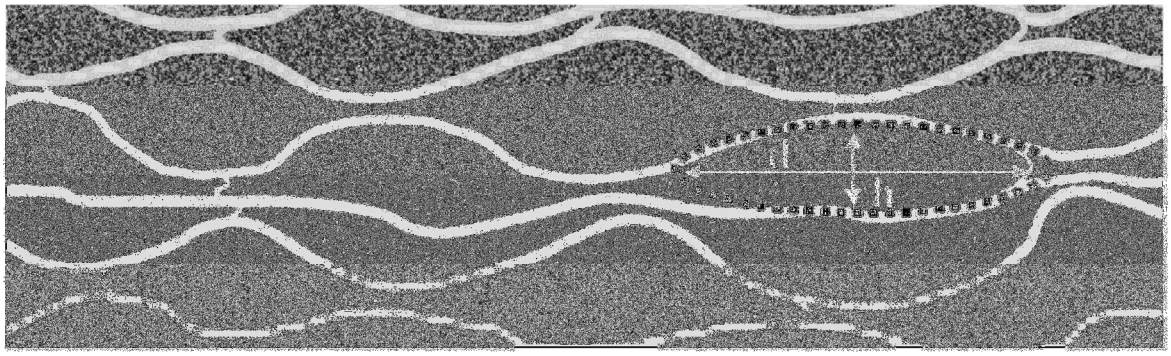

Figure 12. Cross-sectional view of the schematic morphological model for PEDOT:PSS thin films derived from combined STM and X-AFM measurements. Dark PEDOT-rich clusters are separated by lamellas of light PSS. The PEDOT-rich lamella is composed of several pancake-like particles as pictures by the dotted lines. The typical diameter d of the height h is about 5-6nm [41]

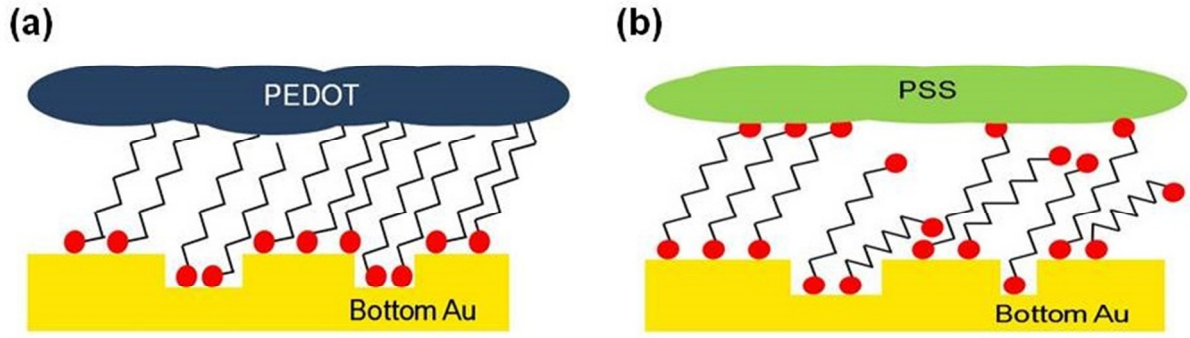

Figure 13. Schematic representation of (a) hydrophobic contact: C8-PEDOT and (b) hydrophilic contact: DC8-PSS

4. CONCLUSION

In this research, octanemonothiol(C8) and octanedithiol(DC8) molecular devices with PEDOT:PSS electrode junction were fabricated and measured as explained in the experiment section. Statistical analysis such as arithmetic, median and Gaussian method were performed on the electric properties measured from PEDOT:PSS C8 and DC8 junction devices. From this analysis, several statistical values were obtained and they show the different electric properties of C8 and DC6. In particular, the average of $Log_{10}J$ of C8 devices was larger than that of DC8 devices and the standard deviation of C8 devices was smaller than that of DC8 devices. The former infers that the conductivity of C8-PEDOT:PSS junction is higher than that of DC8-PEDOT:PSS junction. The latter implies that the molecular contact length of DC8 would be longer than C8. From statistically representative J-V characteristics, we found that the current density of C8 devices is higher than that of DC8 devices by a factor ~10. This result again verifies the different conductivity between C8-PEDOT:PSS junction and DC8-PEDOT:PSS junction. Also this result can be explained by their different contact properties between molecules (C8 and DC8) and PEDOT:PSS interface. That is C8 which have hydrophobic methyl ($-CH_3$) end group adjoin more easily with hydrophobic PEDOT (high conductive) part while DC8 having hydrophilic thiol (-S) adjoin more easily with hydrophilic PSS (less conductive) part in the PEDOT:PSS molecular interfaces. Therefore this different contact (methyl-PEDOT and thiol-PSS) property can be suggested as the reason why the conductivity of C8 devices is higher than that of DC8 devices.

References

[1] S. W. Herwald, S. J. Angello, Science 132, 1127 (1960).

[2] A. Aviram and M. A. Ratner, Chem. Phys. Lett. 29, 277 (1974).

[3] H. B. Akkerman, B. de Boer, J. Phys.: Condens. Matter 20,013001 (2008).

[4] B. Mann, H. Kuhn, J. Appl. Phys. 42, 4398 (1971).

[5] J. K. Tomfohr, O. F. Sankey, Phys. Rev. B 65, 245105 (2002).

[6] A. Salomon , D. Cahen D, S. Lindsay, J. Tomfohr, V. B. Engelkes, C. D. Frisbie, Adv. Mater. 15, 1881 (2003).

[7] H. B. Akkerman, P. W. M. Blom, D. M. de Leeuw, B. de Boer, Nature 441, 69 (2006).

[8] G. Wang, Y. Kim , M. Choe, T.W. Kim, T. Lee, Adv. Mater. 23, 755 (2011).

[9] P. A. Van Hal, E. C. P. Smits, T. C. T. Geuns, H. B. Akkerman, B. C. De Brito, S. Perissinotto, G. Lanzani, A. J. Kronemeijer, V. Geskin, J. Cornil, P. W. M. Blom, B. De Boer, D. M. De Leeuw, Nat. Nanotechnol 3, 749 (2008).

[10] C. A. Nijhuis, W. F. Reus, G. M.Whitesides, J. Am. Chem. Soc. 131, 17814 (2009).

[11] G. Wang, H. Yoo, S.I. Na, T.W. Kim, B. Cho, D.Y. Kim, T. Lee, Thin Solid Films 518, 4 (2009).

[12] S. Datta, W. Tian, S. Hong, R. Reifenberger, J. Henderson, C.P. Kubiak, Phys. Rev. Lett. 79, 2530 (1997).

[13] Y. Xue, S. Datta, M. A. Ratner, J. Chem. Phys. 115, 9, 4292 (2001)

[14] S. Park, *Large area molecular electronic devices on flexible substrate*, Thesis for Master degree, GIST (2012).

[15] P. K. Hansma, Phys. Lett. C Phys. 30, 145 (1977).

[16] C. J. Adkins, W.A. Phillips, J. Phys. C 18, 1313 (1985).

[17] H. Sakaguchi, A. Hirai, F. Iwata, A. Sasaki, T. Nagamura, Appl. Phys. Lett. 79, 3708

(2001).

[18] T. Dadosh, Y. Gordin, R. Krahne, I. Khivrich, D. Mahalu, V. Frydman, I. Bar-Joseph, Nature 436(7051), 677 (2005).

[19] J. C. Love, L. A. Estroff, J. K. Kriebel, R. G. Nuzzo, G. M. Whitesides , Chem. Rev. 105, 1103(2005).

[20] C. Vericat, M. E. Vela , G. A. Benitez , J. A. M. Gago, X. Torrelles, R. C. Salvarezza , J. Phys.: Condens. Matter 18, 867(2006).

[21] P. Maksymovych, D. C. Sorescu, J. T. Jr. Yates, Phys. Rev. Lett. 97, 146103 (2006).

[22] D. Vuillaume, S. Lenfant, Microelectron. Eng. 70, 539 (2003).

[23] B. Xu, N. J. Tao, Science 301, 1221 (2003).

[24] C. C. Kaun, H. Guo, Nano Lett. 3, 1521 (2003).

[25] J. M. Seminario, L. Yan, J. Quant. Chem. 102, 711 (2005).

[26] A. Salomon, D. Cahen, S. Lindsay, J. Tomfohr, V. B. Engelkes, C. D. Frisbie, Adv. Mater. 15 1881 (2003).

[27] X. D. Cui, A. Primak, X. Zarate, J. Tomfohr, O. F. Sankey, A. L. Moore, T. A. Moore, D. Gust, G. Harris, S. M. Lindsay, Science 294, 571 (2001).

[28] Y. Imry, R. Landauer, Rev. Mod. Phys. 71, 306(1999).

[29] V. Mujica, A. Nitzan, S. Datta, M. A. Ratner, C. P. Kubiak , J. Phys. Chem. B 107, 91 (2003).

[30] X. Y. Zhu, J. Phys. Chem. B 108, 8778 (2004).

[31] M. Fujihira, M. Suzuki, S. Fujii, A. Nishikawa, Phys. Chem. Chem. Phys. 8, 3876 (2006).

[32] J. G. Simmons, J. Appl. Phys. 34, 2581 (1963).

[33] W.F. Reus, C.A. Nijhuis, J.R. Barber, M.M. Thuo, S. Tricard, G.M. Whitesides, J. Phys. Chem. C 116, 6714 (2012).

[34] Harold R. Jacobs, Mathematics: A Human Endeavor (3rd ed), W. H. Freeman. (1994).

[35] G. Casella, R. L. Berger, Statistical Inference; Duxbury Press:Belmont, CA (1990).

[36] P.R. Bevington, D.K. Robinson, Data Reduction and Error Analysis for the Physical Sciences (3rd ed), McGraw-Hill, New York (2003).

[37] J.L. Stanford, S.B. Vardeman, Statistical Methods for Physical Science; Methods of Experimental Physics Series 28, Academic Press: San Diego, CA (1994).

[38] P.J. Huber, Robust Statistics; Wiley Series in Probability and Mathematical Statistics; Wiley and Sons: New York, (1981).

[39] L. B. Groenendaal, F. Jonas, D. Freitag, H. Pielartzik, J. R. Reynolds, Adv. Mater. 12, 481 (2000).

[40] S. Kirchmeyer, K. Reuter, J. Mater. Chem. 15, 2077 (2005).

[41] A.M .Nardes, M. Kemerink, R.A.J. Janssen, J. A. M. Bastiaansen, N. M. M. Kiggen, B.M.W.Langeveld, A. J. J. M. van Breemen, M.M. de Kok, Adv. Mater. 19, 1196 (2007).

[42] http://scholarbank.nus.edu.sg/bitstream/handle/10635/25820/XiaYJ.pdf?sequence=1

[43] J. Ouyang, Q. Xu, C. W. Chu, Y. Yang, G. Li, J. Shinar, Polymer 45(25), 8443 (2004).

[44] A. Ulman, An Introduction to Ultrathin Organic Films from Langmuir-Blodgett to Self-Assembly, Academic Press, Boston (1991).

[45] A. Ulman, Chem. Rev. 96, 1533 (1996).

[46] J. Noh, M. Hara, Langmuir 18, 1953 (2002).

[47] C. D. Bain, E. B. Troughton, Y-T. Tao, J. Evall, G. M. Whitesides, and R. G. Nuzzo, J. Am. Chem. Soc. 111, 321 (1989).

[48] S. Park, G. Wang, B. Cho, Y. Kim, S. Song, Y. Ji, M. H. Yoon, T. Lee, Nat. Nanotechnology 7, 438 (2012).

[49] T. W. Kim, G. N. Wang, H. Lee, T. Lee, Nanotechnology 18, 315204 (2007).

[50] J. Taylor, M. Brandbyge, and K. Stokbro, Phys. Rev. Lett. 89, 138301 (2002).

[51] J.L. Vardeman, S.B. Eds, Methods of Experimental Physics Series 28; Academic Press: San-Diego, CA, (1994).

[52] P. J. Rousseeuw, A. M. Leroy, Robust Regression and Outlier Detection; Wiley Series in Probability and Mathematical Statistics; Wiley and Sons: New York, (1987).

[53] H. Yoo, J. Choi, G. Wang, T. W. Kim, J. Noh, T. Lee, Journal of Nanoscience and Nanotechnology 9, 12 (2009).

[54] G. Upton, I. Cook, Understanding Statistics. Oxford University Press, 55 (1996).

[55] D. Zwillinger, S. Kokoska, CRC Standard Probability and Statistics Tables and Formulae, CRC Press, 18 (2000).

[56] K. Seo, H. Lee, ACS Nano 3, 2469 (2009).

국문초록

본 연구에서는 다수의 PEDOT:PSS (3,4-ethylenedioxythiophene) 접합 octanemonothiol(C8)과 octanedithiol(DC8) 분자 소자들이 제작되었으며, 이 소자들로부터 측정된 전기적 특성의 결과에 대하여 통계적 분석이 시행되었다. 각각에 상응하는 통계적 분석 방법들로부터 산술평균, 중앙값, 가우스 평균, 산술 표준편차, 조정 MAD(Median Absolute Deviation) 그리고 가우스 표준편차 등의 다양한 통계 값들을 구할 수 있었으며 또한 Log_{10}(전류 밀도(J)) 히스토그램에 대한 가우스 분포 분석 및 그래프 fitting이 시행되었다. 이어서 각각 C8과 DC8소자들을 대표할 수 있는 통계 값들을 구하고, 이로부터 구하여진 전류밀도-전압(J-V) 특성을 연구하였다. 그리고 이러한 연구로부터 C8 소자의 전기 전도도가 DC8의 그것 보다 약 10배 정도 크다는 것을 알 수 있었다. PEDOT과 PSS의 상이한 특성들로부터, 메틸 말단기를 갖는 C8은 PEDOT과 접하게 되고 싸이올 말단기를 갖는 DC8은 PSS와 접하게 될 것임을 짐작해 볼 수 있었다. 최종적으로 C8과 DC8의 PEDOT:PSS 접합면에서의 차이가 각 분자 소자의 전기 전도도 차이를 불러온다는 것이 이 논문의 결론이다.

Thesis for the degree of Master of Science

이학석사학위논문

Statistical Analysis of electric properties of octanemonothiols and octanedithiols PEDOT:PSS Junctions devices : comparison between the methyl end group and the thiol end group

Octanemonothiol과 Octanedithiol PEDOT:PSS 접합 소자의 전기적 특성에 관한 통계적 분석: 메틸 말단기와 싸이올 말단기간의 비교를 통하여

Hanki Lee

Department of Physics and Astronomy

Seoul National University

서울대학교 대학원

물리천문학부

이 한 기

2014

Abstract

In this study, a large number of octanemonothiol (C8) and octanedithol (DC8) molecular electronic devices with PEDOT:PSS (3,4-ethylenedioxythiophene) interlayer were fabricated and statistical analysis were performed to the electronic properties of these devices. From the analysis, several statistical values such as arithmetic mean, median, Gaussian mean, arithmetic standard deviation, adjusted absolute median deviation, and Gaussian standard deviation were obtained by corresponding methods and also Gaussian plot of histograms of Log_{10}(current density (J)) was fitted by Gaussian methods. Continually the current density–voltage (J-V) characteristics from the statistically representative data for C8 and DC8 devices were investigated and it was, from the investigation, found that the conductivity of C8 is higher than that of DC8 by a factor of ~10. Owing to difference properties of PEDOT and PSS, it can be implied that the C8 with methyl end groups would contact with the PEDOT and DC8 with thiol end groups would contact with the PSS. Finally it is conclusion that the difference of the conductivity of C8 and DC8 with PEDOT:PSS junction devices is originated from the difference of the contact properties between the C8 and DC8 with PEDOT:PSS-interlayer molecular junctions.

Contents

List of Figures

List of Tables

1. Introduction

1.1 Introduction

In 1960, Herwald and Angello stated that 'The trend in electronics circuit construction is toward microminiaturization and molecular electronics.' in their article in 'Science'.[1] In this article, they also supposed that 'the boundaries between materials and devices and between devices and circuits are being removed, and we shall see an integration of disciplines in the future development of molecular electronics.' After 14 years from the prediction, Aviram and Ratner first proposed a method of making a rectifier based on a single organic molecule in 1974.[2] Since the electric properties of molecules can be easily changed by molecular structure and synthesis, molecular electronic devices, in theory, has unlimited possibilities for technological development.[3] Self-assembled monolayer (SAM) is common method in the molecular device fabrication and also popular subject in the field of molecular electronic. In particular SAM of alkanethiol (HS or CH_3-$(CH_2)_n$-SH) ,as were used by Mann and Kuhn[4], are a perfect benchmark for any new experimental testbed in molecular electronics.[3] Because alkanthiols possess a large energy gap between the highest occupied molecular orbital(HOMO) and lowest unoccupied molecular orbital(LUMO) of about 8-10 EV [5,6], these molecules are insulating and, consequently, a tunneling current is expected which decreases exponential with increasing molecule length.[3]

The fabrication of molecular electronic junction using a conductive polymer (PEDOT:PSS; 3,4-ethylenedioxythiophene) between the top electrode and the molecules has been one of the most successful techniques in terms of high device yields and stable junctions. The use of a conducting polymer as a top electrode on top of a SAM in an insulating photoresist matrix

has proven to result in a device with a stability of at least several months in air, no degradation upon sweeping, and working devices with diameters up to 100 μm. Furthermore, the yield of working devices is close to 100% and the technology is compatible with standard integrated circuit fabrication processes.[7] Nevertheless, the use of a conductive polymer presents some uncertainties as a platform for molecular devices because the properties of the interface between the polymer layer and the molecules are not thoroughly understood.[3,7-11] Thus understanding properties of the interface between the polymer layer and the molecules has been crucial demanding task in the field of molecular electronics.

In this study, sufficient number of octanemonothiol (C8; 112 devices) and octanedithol (DC8; 128 devices) molecular devices with PEDOT:PSS interlayer were fabricated for a meaningful statistical analysis which will give an insight to understating properties of the interface. To begin with, the electrical properties of the fabricated molecular devices, current density data from -1V to 1V, were measured and histograms of Log_{10}|current density (J)| was made from them. Several statistical estimates; arithmetic mean (μ_A), median (μ_M), Gaussian mean (μ_G), arithmetic standard deviation (σ_A), adjusted absolute median deviation (σ_M), and Gaussian standard deviation (σ_G) could be obtained and analyzed statistically. Next the conductivity of C8 devices and the conductivity of DC8 devices were studied once more by comparing their current density-voltage (J-V) characteristics from representative data. Also, refer to the characteristics of PEDOT and PSS studied in proceeding research, the relation between octanethiol's end groups (Methyl and Thiol) with the PEDOT:PSS was suggested to understand the interface properties. Finally the relation between the conductivity and the contact properties in molecule-PEDOT:PSS interface was discussed to understand the difference in the electrical characteristics

1.2 Conduction mechanism through Molecular Junctions

In a molecular junction, the Fermi level alignment is critical in determining the conduction mechanism.[12] Created by the overlap of the atomic orbitals of a molecule's constituents, two molecular orbitals, lowest unoccupied molecular orbital (LUMO) and highest occupied molecular orbital (HOMO), play similar role as a conduction band and valence band in a semiconductor, respectively. The Fermi level of the metallic contacts generally does not align with either the HOMO or the LUMO of the molecule, but instead lies close to the center of the gap.[13] This energy level mismatch gives rise to a contact barrier, including a height and a thickness of this barrier and the presence of defects.[14]

There are various models to explain conduction mechanism which have their characteristic behavior, temperature dependence, and voltage dependence; 1) Direct Tunneling 2) Fowler-Nordheim Tunneling 3) Thermionic Emission and 4) Hopping conduction. Here we focus on direct tunneling as main conduction mechanism in molecular electric devices made with short length (< 1-2 nm) of molecules. Figure 1 is an energy band diagram describing the quantum mechanical tunneling through a thin gap. In this diagram, positive voltage is applied to the right side electrode, thus the Fermi energy of the right electrode is lowered with respect to the left side. The potential barrier Φ_B is formed by the gap (molecule in this case) between the left and right side electrodes. When an electron from occupied states on the left side tunnels into empty states on the right side, one can consider two types of direct tunneling; elastic tunneling and inelastic tunneling. In the elastic tunneling, the energy of the tunneling electron from left to right side is conserved whereas that is not conserved in the inelastic tunneling. In the inelastic tunneling, the lost energy from the tunneling electron transfers to molecular vibrational modes. This electron-vibration mode coupling occurs at characteristic frequency ω of molecular vibration modes.[15,16] Only elastic tunneling is considered for simple

discussion in this study.

Coherent and incoherent tunneling have been two distinct transport mechanism which were extensively discussed in the literature.[17,18] I-V characteristics as a function of temperature and molecular length are essential to identify the conduction mechanism; Coherent tunneling is typified by a temperature independent. On the contrary, incoherent tunneling is characterized by a weak length dependent. Coherent tunneling dominates in short molecules. In the contrast, incoherent tunneling occurs along long-conjugated molecular wires. Following equations represent the character of coherent tunneling. According to this equation, the conductance value (G) decreases exponentially as the molecular length increases.

$$G \propto \exp(-\beta d) \qquad (1)$$

Here, d is the molecular length and β is the tunneling decay coefficient.

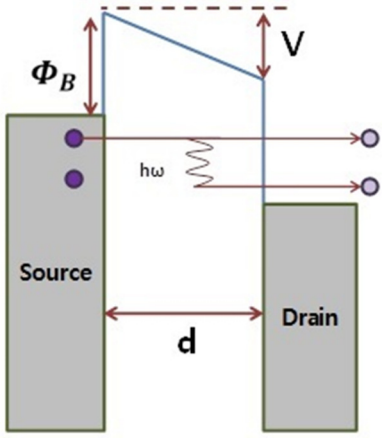

Figure 1. A schematic Energy band diagram of a molecular junction

1.3. The molecule-electrode interface

The interface between the molecules and the electrodes can be divided into chemisorbed or physisorbed contact.[19] Not fully understood yet, the formation of Au–S bond has known to be a chemisorbed contact.[19~22] The difference between a chemisorbed contact and a physical contact can lead to a change of a few orders of magnitude in conductivity of the junction.[23-25] In the case of alkanethiol molecules, this difference in conductivity between physisorbed and chemisorbed contacts can be understood by describing current through the molecular junction with the Landauer formula [25-31], stating that the conductance G is given by:

$$\mathrm{G} = \frac{2e^2}{h} \times T_b \times T_{mol} \times T_t \qquad (2)$$

where e is the elementary charge, h is the Planck's constant and T_b, T_t and T_{mol} are the transmission coefficients of the bottom interlayer contact, top interlayer contact and the molecule, respectively. From this formula, it can be inferred that a change in transmission of any contacts will alter the absolute value of the conductance with the same factor. Thus, to make a good comparison between the obtained currents per molecule, the differences in transmission of the second contact must be accounted for. One prime example is the contact difference between alkanemonothiols and alkanedithiols.[3] In this study, we compare the contact difference between octanemonothiols and octanedithiols with PEDOT:PSS interlayer.

1.4 Statistical Analysis method

Simmons model [32] is used as an initial point to start our statistical analysis. When the Simmons model holds, current density (J) depends exponentially on molecular contact length (d) as followed;

$$J \propto \exp(-\beta d);\ \text{where } \beta \text{ is the tunneling decay constant.}$$

Thus a normal distribution of d would translate to a normal distribution of Log |J/(A/cm2)|, simply log|J|.[33] Normal distribution is so called Gaussian distribution and defined by following equation;

$$f(x) = \frac{1}{\sigma_G \sqrt{2\pi}} exp\left[\frac{(x-\mu_G)^2}{2{\sigma_G}^2}\right] \qquad (3)$$

where μ_G is the Gaussian mean and σ_G is the Gaussian standard deviation. The accuracy of the Gaussian mean and standard deviation depends heavily whether all informative measurements of log|J| are randomly sampled from a normal distribution.[33]

For more ample statistical analysis, following methods were also performed in this paper.

(1) Arithmetic mean and standard deviation

Arithmetic mean (μ_A) is the sum of a collection of numbers divided by the number of numbers in the collection.[33] Arithmetic standard deviation (σ_A) is the square root of second moment about μ_A.[34]

(2) Median and median absolute deviation

The median (μ_M) is defined [35-37] as the value for which 50% of the sample is greater than or equal to that value, and 50% of the sample is less than or equal to that value. Though median absolute deviation is useful for visualizing sample, it can't be compared directly like σ_G and σ_A. However, for comparison with them, we can use the following adjusted median absolute deviation (σ_M) as demoted; [38]

$$\sigma_M = 1.4826 \times \text{median}(|x - \mu_M|) \qquad (4)$$

The quantity, median ($|x-\mu_M|$), is called the median absolute deviation, and the factor of 1.4826 adjusts this quantity to correct for underestimation of the sample standard deviation.

2. Experiment

2.1 Conducting Polymer: PEDOT:PSS (3,4-ethylenedioxythiophene)

PEDOT:PSS is a polymer mixture of two ionomers; PEDOT and PSS. PEDOT(chemical structure shown in Figure 2) is a derivative of polythiophene and is usually prepared by polymerization of ethylenedioxythiophene (EDOT). Conductive PEDOT can be prepared by electrochemical or chemical polymerization. PEDOT doped with small anions are insoluble in any solvent. When excess PSS (chemical structure shown in Figure 2) is used as the counter anion for the PEDOT by chemical oxidation, however, PEDOT:PSS can be dispersed in water. The PEDOT chains are attached to the PSS chains through the Coulombic interaction. They are stabilized by the excess PSS. In other words, the excess PSS is used to stabilize PEDOT in water; i.e. the hydrophilic PSS chains form micelles with the hydrophobic PEDOT chains inside. Briefly PEDOT:PSS is a blend of an oxidatively doped, cationic, conducting polythiophene derivative (PEDOT) that is electrostatically bound to a PSS polyanion. PEDOT:PSS combines high conductivity and good transparency in the visible region with excellent stability under ambient conditions and can be easily processed from aqueous dispersions by spin coating.[39-42]

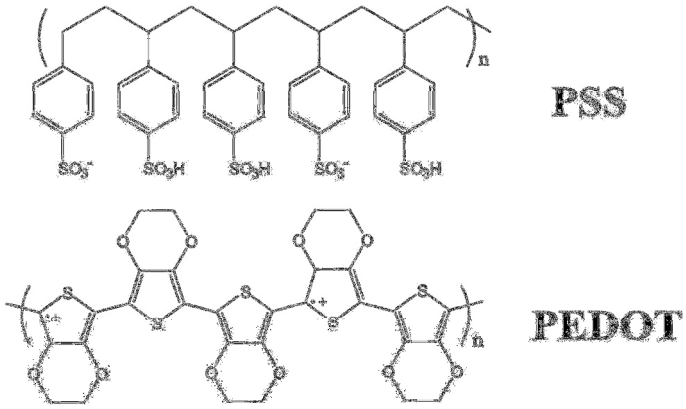

Figure 2. Chemical Structure of PEDOT:PSS [43]

2.2 Self Assembled Monolayer (SAM): Octanemonothiols(C8) and Octanedithiols(DC8)

Octanemonothiol(C8) is a one side's thiol-terminated eight-alkyl chain molecular system ; CH_3-$(CH_2)_8$-SH] and Octanedithiol(DC8) is a both sides thiol-terminated eight-alkyl chain molecular system ; HS-$(CH_2)_8$-SH. As commonly known, self-assembled alkanethiols on Au surface form densely packed and crystalline-like structure with the alkyl chain in an all-trans conformation. [44] The Self Assembled Monolayer (SAM) process is can be explained by following chemical reaction [45,46]

$$R\text{-}SH + Au \rightarrow RS\text{-}Au + o.5\ H_2 \qquad (5)$$

where R is the backbone of the molecule and -SH is a thiol end. This chemical absorption process is indicated to two steps: 1) a swift process that takes minutes (depending on the thiol concentration) and gives ~ 90% of the film thickness 2) a gradual process that lasts hours and reaches the final thickness and contact angle.[44,46] There are three forces suggested to determine this SAM process and the final monolayer structure: the interaction between the thiol head group and gold lattice, dispersion force between alkyl chains (van der Waals force, etc.), and the interaction between the end groups.[47]

Figure 2 shows molecular structures of octanemonothiol (C8) and octanedithiol (DC8) in PEDOT:PSS junction. In the bottom surface, both thiol end groups are chemisorbed with the Au surface in both structures. In the top surface, however, methyl end groups of C8 contact with the PEDOT:PSS junction and thiol end groups of DC8 contact with the PEDOT:PSS junction.

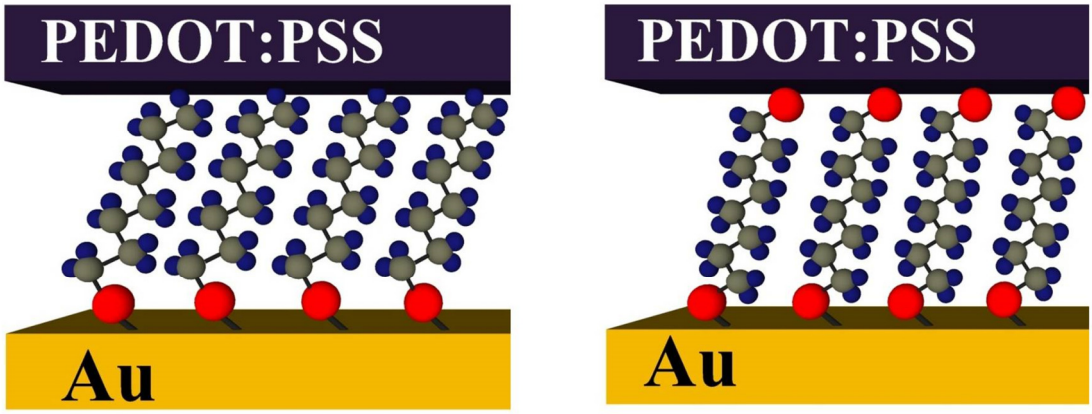

a. Octanemonothiol(C8)

b. Octanedithiol(DC8)

Figure 3. Molecular Structures of C8 and DC8 in PEDOT:PSS Junction

2.3 Device Fabrication

The PEDOT:PSS molecular junction devices (Au-Octanethiol-PEDOT:PSS/Au) fabrication procedures are shown in Figure 3. First, designed Au (500 Å)/Ti (100 Å) bottom electrodes were deposited on a p-type (100) 300 nm thickness SiO_2 substrate using a shadow mask by an electron beam evaporator at a rate of ~0.1 Å/s. Then photoresist (AZ5214) was spin coated on the bottom electrodes to form an insulating wall which electrically isolates the bottom electrodes with the top electrodes. Next the UV photolithography process was performed to make hole structures in the photoresist layer by a mask aligner. The holes were square-shaped and had side lengths ranged from 30 μm to 100 μm with an increment of 10 μm. After the formation of the via-hole pattern, the devices were annealed on a hot plate at ~200 ^{o}C for 2 h 30 min to make the photoresist layer insoluble in ethanol during the formation of the molecular self-assembled monolayer (SAM) on the bottom electrodes. Next the devices were put into 2 mM octanemonothiol (C8) and octanedithiol (DC8) solutions diluted with ethanol to form the SAM on the bottom electrodes for 24hours~48hours. After the SAM process, the devices were rinsed with ethanol to remove residual unbounded molecules. Subsequently PEDOT:PSS was spin coated on the devices for 3 minutes and dried for 3 hours. SAM forming, PEDOT:PSS coating and drying process were all performed in the N^2 gas filled glove box Chamber and at the room temperature. And Au top electrodes (500 Å) were deposited on top of the PEDOT:PSS interlayer using a shadow mask by an electron beam evaporator at a rate of ~0.1 Å/s. To prevent the formation of a direct current path through the PEDOT:PSS layer between the top and bottom Au electrodes, reactive ion etching (RIE) was finally performed with O_2 gas to remove redundant PEDOT:PSS layers on the devices.[48] Figure 4 is the schematic diagram of the device structure of the PEDOT:PSS junction molecular devices. The J-V characteristics of the fabricated devices were measured

by using a semiconductor parameter analyzer (Keithley 4200-SCS) in N^2 gas filled glove box to prevent the degradation by water vapor and O2.

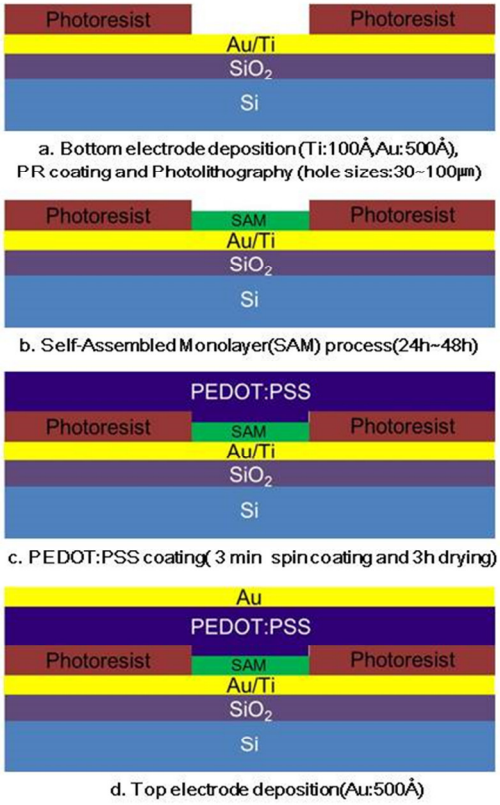

Figure 4. Device Fabrication Procedures of PEDOT:PSS Molecular Junction Devices

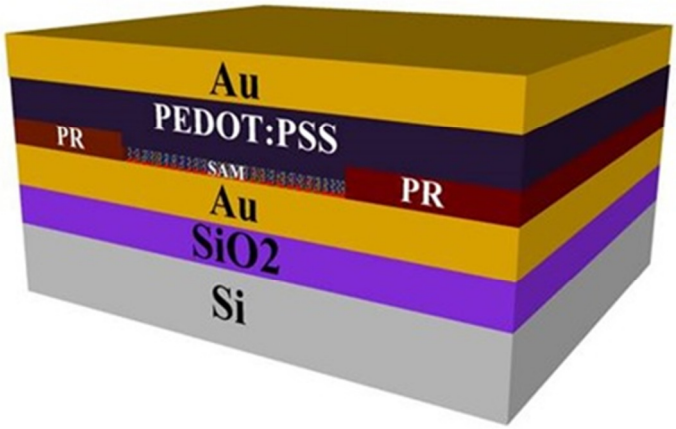

Figure 5. A schematic diagram of the PEDOT:PSS Molecular Junction Device Structure

3. RESULTS AND DISCUSSION

3.1 Statistical analysis of an electric property of C8 and DC8 molecular devices

The statistical approach to molecular electronic devices can provide a useful way to distinguish the transport property of different molecular system.[49] Sufficient number of devices which give trustworthy information are necessary to conduct the statistical analysis. Hence numerous number of device fabrication has been suggested as an initial condition for the analysis in many preceding research. In addition enough yields of 'working' devices are also suggested for the successful analysis. Working devices might be typically defined as a device showing non-linear I-V behavior and not being electrical open and short. Open devices are noisy with a current level normally in pA degree and short devices show Ohmic(linear) I-V characteristics with a current level larger than a few mA.[50]

Accordingly each 112 C8 devices and 128 DC8 devices were fabricated for the statistical analysis in this research. Also, from the above defining criteria, 61 C8 devices and 89 DC8 devices could be selected as working devices. However above mentioned criteria is just basic standard to define informative devices which give valuable data for the statistical analysis. Among the raw working devices, informative devices are still to be distinguished with the non-informative devices by performing certain methodology. There are two major ways to draw a distinction between informative and non-informative data: (1) construct a parametric statistical model [35,36,51] that assumes that informative devices follow a certain probability distribution, while non-informative devices follow a different distribution, or (2) assume that the majority of devices are informative and choose a methodology that is insensitive to

relatively small numbers of extreme data (that is, a "robust" method [38,52]) since these devices are likely to be non-informative.

In this research, the 'informative' working devices were extracted from the devices showing a majority of current densities in the statistical distribution by using a Gaussian distribution function.[53] Precisely 99.7% of the devices from overall population which were included in the interval of the $3\sigma_G$ range between $\mu_G + 3\sigma_G$ and $\mu_G - 3\sigma_G$ were selected as the 'informative' working devices.[49] Figure 5 and 6 show the histograms of $Log_{10}J$ of 'raw' working devices of molecular devices and also their denoted 3 σ_G ranges. First, in figure 5, 61 working C8 devices were in $3\sigma_G$ ranges (99.7% ranges) so selected as the informative. Next, in Figure 6, 89 working DC8 working devices were also in $3\sigma_G$ ranges so selected as same. Outliers (data that lie far from the peak in histograms of $Log_{10}J$) and long tails (larger share of the data to the right of the peak than in a normal distribution) [33] which suggested to be 'non-informative' were excluded by this process. Finally the device yield of 'informative' working devices was each 57/112 = 50.9% for C8 devices and 86/128 = 67.2% for DC8 devices in PEDOT:PSS-electrode molecular junction structure. This yield is significantly larger as compared with the case of metal-molecule-metal junction structure without using PEDOT:PSS interlayer which showed a typical device yield of ~1%.[49] Both histograms were fitted with the Gaussian distribution function (See 1.3 section) and the curves in the figures are the results of this fitting. And figure 7 is the integrated histograms of $Log_{10}J$ of 'informative' working devices of C8 and DC8 molecular. The directed positions in figure 7 by arrows are the Gaussian mean of each distribution and they imply that the $Log_{10}J$ of C8 is slightly larger than that of DC8.

To compare data of C8 and DC8 devices more specifically, statistical methods explained in Section 1.4 were used in this research; 1) Arithmetic 2) Median 3) Gaussian. (Details of each method are explained in Section 1.4.)

Table 1 shows the results from those statistical methods performed to C8 and DC8 PEDOT:PSS junction devices. First the arithmetic mean (μ_A) of C8 and DC8 devices is each 1.24 and 0.77. Next the median (μ_M) of C8 and DC8 devices is each 1.34 and 0.81. And the Gaussian mean (μ_G) of C8 and DC8 devices is each 1.37 and 0.83. As summarized, μ_G of C8 and DC8 molecular devices is found to be larger than μ_A of them by 0.13 and 0.06, respectively. However, μ_G of C8 and DC8 devices is larger than μ_M only by 0.03 and 0.02, respectively. Overall the current density of C8 devices is larger than that of DC8 devices and this fact implies that the conductivity of PEDOT:PSS-C8 molecular devices is higher than that of PEDOT:PSS-DC8 molecular devices. Now compare the standard deviation of each molecular device. First the Arithmetic standard deviation (σ_A) of C8 and DC8 is each 0.56 and 0.66. Next the adjusted absolute median deviation (σ_M) of C8 and DC8 devices is 0.31 and 0.57. And the Gaussian standard deviation (σ_G) of C8 and DC8 devices is each 0.30 and 0.51. In other words, σ_G of C8 and DC8 devices are found to be smaller than σ_A of C8 and DC8 devices by 0.26 and 0.15, respectively. But σ_G of C8 and DC8 devices are smaller than σ_A of C8 and DC8 devices only by 0.01 and 0.06, respectively. Overall the standard deviation of C8 devices is smaller than that of DC8 devices. Because the distributions of $Log_{10}J$ coincide with distribution of molecular contact length from Simmons model [32] and the standard deviation of d is normally proportional to the size of it, the larger standard deviation means the longer molecular length. Therefore the larger standard deviation of DC8 devices implies the longer molecular length of DC8 molecular junction. In other words, the molecular contact length of PEDOT:PSS-DC8 junction might be longer than that of PEDOT:PSS-C8 junction.

From above, we can find that the difference between the arithmetic and Gaussian statistical values of two devices are much larger than that between the median and Gaussian values of them. These results are because μ_A and σ_A respond strongly to long tails (larger share of the

data to the right of the peak than in a normal distribution) and outliers (data that lie far from the peak in histograms of $Log_{10}J$). Since most histograms had long tails and outliers, σ_A was usually found to be greater than σ_G.[33]

For a true normal distribution, it is has been known that any estimates of the standard deviation will tend to be smaller than interquartile range (IQR) which is equal to the difference between the upper and lower quartiles.[54-55] In this research, IQR of C8 and DC8 molecular devices were found to be 0.40 and 0.80, respectively. Comparing them with standard deviation results in Table 1, all standard deviation values of DC8 devices are smaller than its IQR value. Also σ_M and σ_G of C8 devices are smaller than its IQR value. However, due to outliers shown in figure 5, σ_A is not smaller than the IQR value.

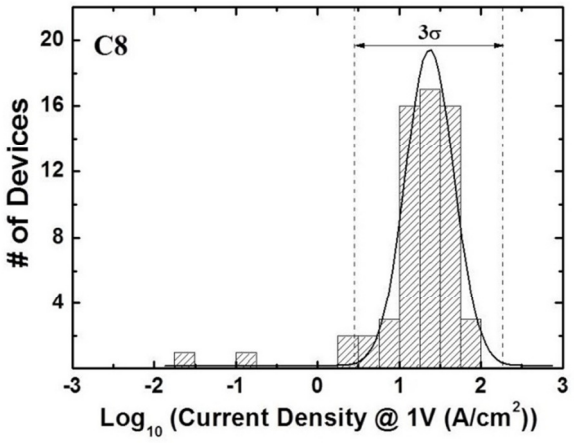

Figure 6. Histogram of logarithmic current devices at 1 V from 'raw' C8 molecular working devices

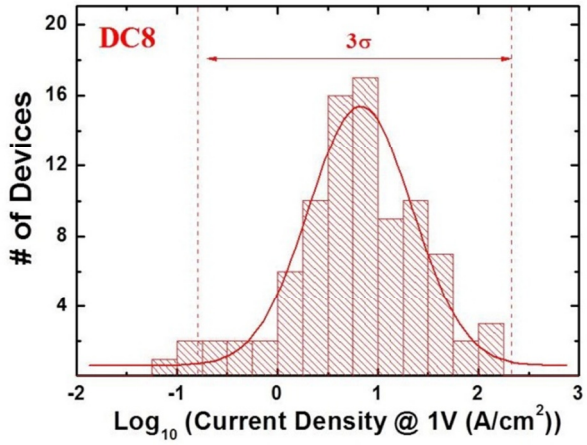

Figure 7. Histogram of logarithmic current devices at 1 V from 'raw' DC8 molecular working devices

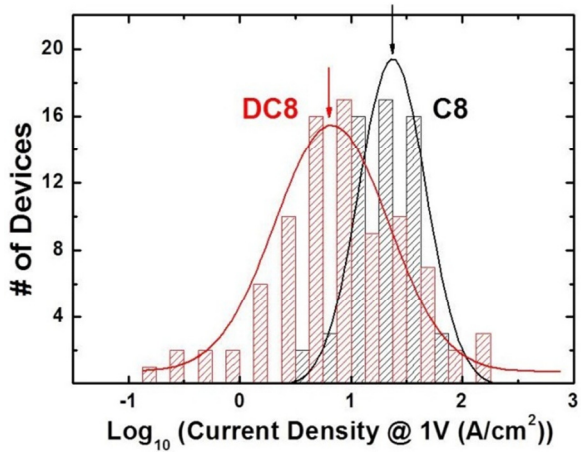

Figure 8. Histogram of logarithmic current densities at 1 V for 'informative' C8 and DC8 working devices.

	μ_A	μ_M	μ_G	σ_A	σ_M	σ_G
C8	1.24	1.34	1.37	0.56	0.31	0.30
DC8	0.77	0.81	0.83	0.66	0.57	0.51

Table1. The list of statistical estimates for C8 and DC8 molecular devices

Note: μ_A: arithmetic mean, μ_M: median, μ_G: Gaussian mean, σ_A: arithmetic standard deviation, σ_M: adjusted absolute median deviation, σ_G: Gaussian standard deviation. The unit of μ_A, μ_M and μ_G is $Log_{10}(A/cm^2)$.

3.2 The electric properties from different contact interface between C8 and DC8 with PEDOT:PSS junctions

Current density reflects the conductivity of different molecular systems.[49] Here the data near from the median of Log_{10} J (see Table 1)were collected as statistical representatives and plotted to current density-Voltage(J-V) characteristics. Figure 8 shows J-V characteristic of C8 and DC8 molecular devices. The plot of C8 devices is clearly distinguished from the plot of DC8 devices. Numerically the J of C8 representative junction is higher than that of DC8 representative junction by a factor of ~10 in the A/cm^2 unit.

These different conductivities of C8 and DC8 representative devices are related to their different contact interfaces with PEDOT:PSS electrodes. As mentioned in Section 1.3, the electrode-molecule interface can be divided into a chemisorbed or physisorbed contact. In this Au-Molecule-PEDOT:PSS junction, the interface of DC8 SAM on the bottom Au (111) has the same ordering structure (tilt angle and packing density) as the C8 SAM on Au(111) .[56] Because the head thiol group of C8 and DC8 will make identical chemisorbed contact with the bottom Au electrode in the same chemical reaction explained in Section 2.2. But the interface of DC8 SAM with the top PEDOT:PSS is different to the interface of C8 SAM with the PEDOT:PSS. Since the thiol end-group of DC8 (-S) contact with the PEDOT:PSS electrode while methyl end-group of C8 ($-CH_3$) contact with the PEDOT:PSS electrode. Thus possible reason of their different conductivities can be originated from their different interface between C8 and DC8 with the PEDOT:PSS junctions. To investigate above assumption more precisely, the research on spin coated PEDOT:PSS has to be studied.

Figure 9 and 10 show the topographic scanning tunneling microscopy (STM) image and cross-sectional (atomic force microscopy) AFM phase image of PEDOT:PSS film. First, Figure 9 shows that PEDOT:PSS films indeed have a granular morphology, with a typical

grain size of about 20~25nm. These grains are also suggested to have the shape of pancake-like structure. Next Figure 10 can be interpreted as side view of PEDOT-rich "pancakes" (dark features) with a thickness of a few nanometers and a diameter of a few tens of nanometers separated by PSS lamellas (bright features). In the normal direction, the separating barriers, that is, the PSS lamellas are quasi-continuous, whereas the separations in the lateral direction do not seem to be fully closed. Clearly, a top view of these lasagna-like structures should look like Figure 9. These STM and X-AFM measurements can be combined into the schematic morphological model as shown in Figure 11. Figre 11 shows that PEDOT-rich clusters (dark) are separated by lamellas of PSS (light) and pancake-like particles as pictured by the dotted lines. Also PEDOT-rich core has a much higher intrinsic conductivity than the PEDOT-depleted grain boundary, which is essentially insulating because PSS is a weak ionic conductor. In other words, due to the fact that PEDOT is a high conductor whereas PSS is a weak one, the current is more easily transported through the PEDOT-rich area than PSS lamellas.[42] Therefore, in the PEDOT:PSS molecular junction, it can be suggested that the conductivity of the junction will be higher when molecules make contact with PEDOT-rich area rather than PSS.

In the Au -C8/DC8-PEDOT:PSS junction, C8 and DC8 make contacts with the bottom electrodes with thiol end group (-S), but the other end of C8 and DC8 which are coated with PEDOT:PSS makes different contacts due to the end group of each type of molecules; i.e. C8 has hydrophobic methyl ($-CH_3$) as the end group whereas DC8 has hydrophilic thiol (-S) as the end group. Though PEDOT:PSS is water-soluble and hydrophilic, PEDOT is itself hydrophobic and PSS is hydrophilic as mentioned in Section 2.1. From this reason, it can be inferred that the hydrophobic methyl end group of C8 would prefer to make contact with hydrophobic PEDOT area than hydrophilic PSS lamellas. Whereas, compared to the C8 case, the hydrophilic thiol end group of DC8 would contact more easily with hydrophilic PSS

lamellas than hydrophobic PEDOT region. Because both thiol and methyl makes physisorbed contact with PEDOT:PSS and , in this case , hydrophobic materials adjoin easily with same nature materials while hydrophilic one do in the same manner. Thus these different contact (methyl-PEDOT and thiol-PSS) properties can explain why the conductivity of C8 devices is higher than that of DC8 devices. Figure 12 shows the schematic representations of C8 with hydrophobic methyl contact to high conducting PEDOT part and DC8 with hydrophilic thiol contact to weak conducting PSS part. Refer to the Landauer model shown in Sec 1.3, the change in the transmission coefficient of top interlayer contact (Here Methyl-PEDOT:PSS and Thiol-PEDOT:PSS) makes different conductivity between the C8 and DC8 devices.

To conclude, PEDOT:PSS-C8 junctions show higher conductivity than PEDOT:PSS-DC8 junctions in that C8 having hydrophobic methyl end groups would smoothly connect to high conducting and hydrophobic PEDOT regions while DC8 which has hydrophilic thiol end groups would smoothly contact with weak conducting and hydrophilic PSS lamellas.

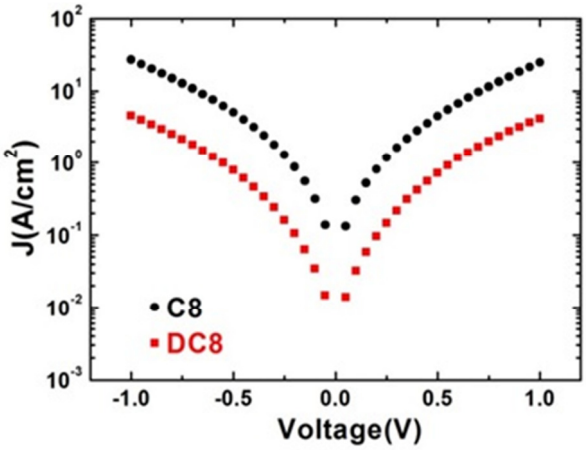

Figure 9. Current density-Voltage (J-V) characteristics of representative C8 and DC8 PEDOT:PSS junction devices

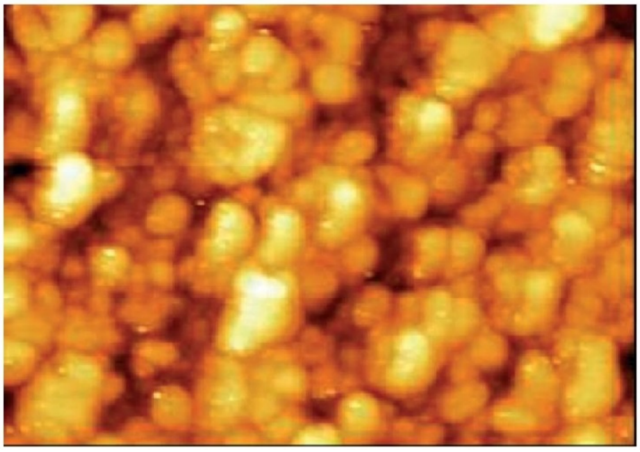

Figure 10. The topographic STM image of PEDOT:PSS on indium tin oxide(ITO) at 2.3V, tunneling current 10pA [41]

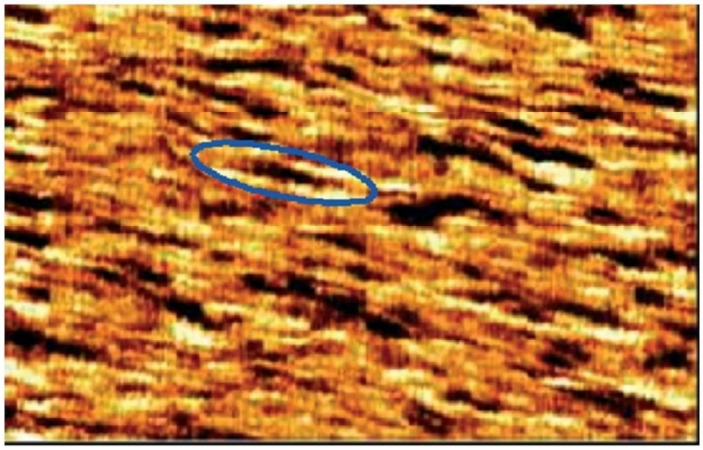

Figure 11. The cross-sectional AFM phase image of cleaved PEDOT:PSS on glass. A pancake like particle is highlighted by the ellipse [41]

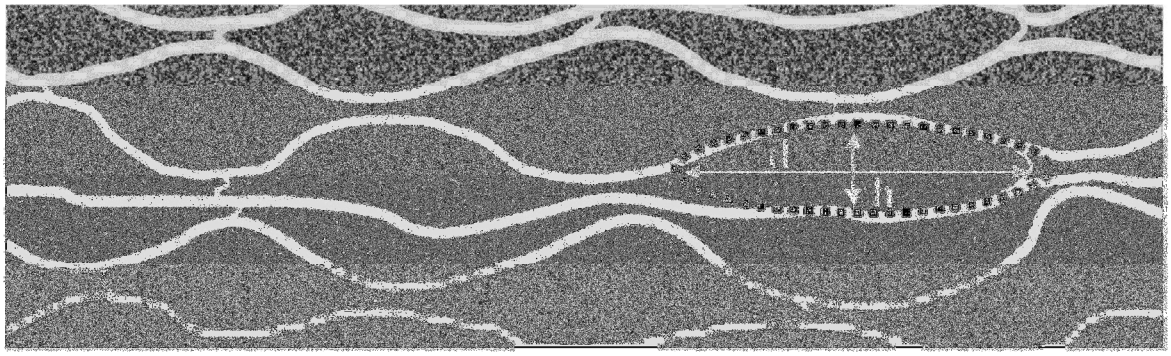

Figure 12. Cross-sectional view of the schematic morphological model for PEDOT:PSS thin films derived from combined STM and X-AFM measurements. Dark PEDOT-rich clusters are separated by lamellas of light PSS. The PEDOT-rich lamella is composed of several pancake-like particles as pictures by the dotted lines. The typical diameter d of the height h is about 5-6nm [41]

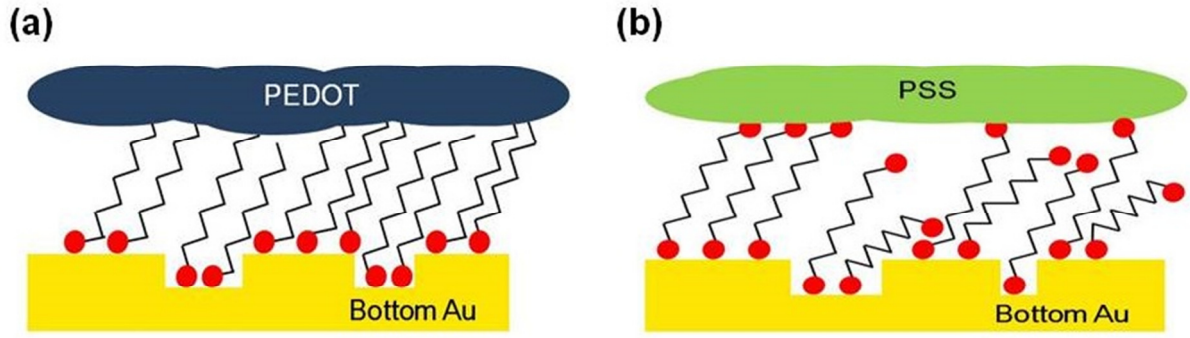

Figure 13. Schematic representation of (a) hydrophobic contact: C8-PEDOT and (b) hydrophilic contact: DC8-PSS

4. CONCLUSION

In this research, octanemonothiol(C8) and octanedithiol(DC8) molecular devices with PEDOT:PSS electrode junction were fabricated and measured as explained in the experiment section. Statistical analysis such as arithmetic, median and Gaussian method were performed on the electric properties measured from PEDOT:PSS C8 and DC8 junction devices. From this analysis, several statistical values were obtained and they show the different electric properties of C8 and DC6. In particular, the average of $Log_{10}J$ of C8 devices was larger than that of DC8 devices and the standard deviation of C8 devices was smaller than that of DC8 devices. The former infers that the conductivity of C8-PEDOT:PSS junction is higher than that of DC8-PEDOT:PSS junction. The latter implies that the molecular contact length of DC8 would be longer than C8. From statistically representative J-V characteristics, we found that the current density of C8 devices is higher than that of DC8 devices by a factor ~10. This result again verifies the different conductivity between C8-PEDOT:PSS junction and DC8-PEDOT:PSS junction. Also this result can be explained by their different contact properties between molecules (C8 and DC8) and PEDOT:PSS interface. That is C8 which have hydrophobic methyl ($-CH_3$) end group adjoin more easily with hydrophobic PEDOT (high conductive) part while DC8 having hydrophilic thiol (-S) adjoin more easily with hydrophilic PSS (less conductive) part in the PEDOT:PSS molecular interfaces. Therefore this different contact (methyl-PEDOT and thiol-PSS) property can be suggested as the reason why the conductivity of C8 devices is higher than that of DC8 devices.

References

[1] S. W. Herwald, S. J. Angello, Science 132, 1127 (1960).

[2] A. Aviram and M. A. Ratner, Chem. Phys. Lett. 29, 277 (1974).

[3] H. B. Akkerman, B. de Boer, J. Phys.: Condens. Matter 20,013001 (2008).

[4] B. Mann, H. Kuhn, J. Appl. Phys. 42, 4398 (1971).

[5] J. K. Tomfohr, O. F. Sankey, Phys. Rev. B 65, 245105 (2002).

[6] A. Salomon , D. Cahen D, S. Lindsay, J. Tomfohr, V. B. Engelkes, C. D. Frisbie, Adv. Mater. 15, 1881 (2003).

[7] H. B. Akkerman, P. W. M. Blom, D. M. de Leeuw, B. de Boer, Nature 441, 69 (2006).

[8] G. Wang, Y. Kim , M. Choe, T.W. Kim, T. Lee, Adv. Mater. 23, 755 (2011).

[9] P. A. Van Hal, E. C. P. Smits, T. C. T. Geuns, H. B. Akkerman, B. C. De Brito, S. Perissinotto, G. Lanzani, A. J. Kronemeijer, V. Geskin, J. Cornil, P. W. M. Blom, B. De Boer, D. M. De Leeuw, Nat. Nanotechnol 3, 749 (2008).

[10] C. A. Nijhuis, W. F. Reus, G. M.Whitesides, J. Am. Chem. Soc. 131, 17814 (2009).

[11] G. Wang, H. Yoo, S.I. Na, T.W. Kim, B. Cho, D.Y. Kim, T. Lee, Thin Solid Films 518, 4 (2009).

[12] S. Datta, W. Tian, S. Hong, R. Reifenberger, J. Henderson, C.P. Kubiak, Phys. Rev. Lett. 79, 2530 (1997).

[13] Y. Xue, S. Datta, M. A. Ratner, J. Chem. Phys. 115, 9, 4292 (2001)

[14] S. Park, *Large area molecular electronic devices on flexible substrate*, Thesis for Master degree, GIST (2012).

[15] P. K. Hansma, Phys. Lett. C Phys. 30, 145 (1977).

[16] C. J. Adkins, W.A. Phillips, J. Phys. C 18, 1313 (1985).

[17] H. Sakaguchi, A. Hirai, F. Iwata, A. Sasaki, T. Nagamura, Appl. Phys. Lett. 79, 3708

(2001).

[18] T. Dadosh, Y. Gordin, R. Krahne, I. Khivrich, D. Mahalu, V. Frydman, I. Bar-Joseph, Nature 436(7051), 677 (2005).

[19] J. C. Love, L. A. Estroff, J. K. Kriebel, R. G. Nuzzo, G. M. Whitesides , Chem. Rev. 105, 1103(2005).

[20] C. Vericat, M. E. Vela , G. A. Benitez , J. A. M. Gago, X. Torrelles, R. C. Salvarezza , J. Phys.: Condens. Matter 18, 867(2006).

[21] P. Maksymovych, D. C. Sorescu, J. T. Jr. Yates, Phys. Rev. Lett. 97, 146103 (2006).

[22] D. Vuillaume, S. Lenfant, Microelectron. Eng. 70, 539 (2003).

[23] B. Xu, N. J. Tao, Science 301, 1221 (2003).

[24] C. C. Kaun, H. Guo, Nano Lett. 3, 1521 (2003).

[25] J. M. Seminario, L. Yan, J. Quant. Chem. 102, 711 (2005).

[26] A. Salomon, D. Cahen, S. Lindsay, J. Tomfohr, V. B. Engelkes, C. D. Frisbie, Adv. Mater. 15 1881 (2003).

[27] X. D. Cui, A. Primak, X. Zarate, J. Tomfohr, O. F. Sankey, A. L. Moore, T. A. Moore, D. Gust, G. Harris, S. M. Lindsay, Science 294, 571 (2001).

[28] Y. Imry, R. Landauer, Rev. Mod. Phys. 71, 306(1999).

[29] V. Mujica, A. Nitzan, S. Datta, M. A. Ratner, C. P. Kubiak , J. Phys. Chem. B 107, 91 (2003).

[30] X. Y. Zhu, J. Phys. Chem. B 108, 8778 (2004).

[31] M. Fujihira, M. Suzuki, S. Fujii, A. Nishikawa, Phys. Chem. Chem. Phys. 8, 3876 (2006).

[32] J. G. Simmons, J. Appl. Phys. 34, 2581 (1963).

[33] W.F. Reus, C.A. Nijhuis, J.R. Barber, M.M. Thuo, S. Tricard, G.M. Whitesides, J. Phys. Chem. C 116, 6714 (2012).

[34] Harold R. Jacobs, Mathematics: A Human Endeavor (3rd ed), W. H. Freeman. (1994).

[35] G. Casella, R. L. Berger, Statistical Inference; Duxbury Press:Belmont, CA (1990).

[36] P.R. Bevington, D.K. Robinson, Data Reduction and Error Analysis for the Physical Sciences (3rd ed), McGraw-Hill, New York (2003).

[37] J.L. Stanford, S.B. Vardeman, Statistical Methods for Physical Science; Methods of Experimental Physics Series 28, Academic Press: San Diego, CA (1994).

[38] P.J. Huber, Robust Statistics; Wiley Series in Probability and Mathematical Statistics; Wiley and Sons: New York, (1981).

[39] L. B. Groenendaal, F. Jonas, D. Freitag, H. Pielartzik, J. R. Reynolds, Adv. Mater. 12, 481 (2000).

[40] S. Kirchmeyer, K. Reuter, J. Mater. Chem. 15, 2077 (2005).

[41] A.M .Nardes, M. Kemerink, R.A.J. Janssen, J. A. M. Bastiaansen, N. M. M. Kiggen, B.M.W.Langeveld, A. J. J. M. van Breemen, M.M. de Kok, Adv. Mater. 19, 1196 (2007).

[42] http://scholarbank.nus.edu.sg/bitstream/handle/10635/25820/XiaYJ.pdf?sequence=1

[43] J. Ouyang, Q. Xu, C. W. Chu, Y. Yang, G. Li, J. Shinar, Polymer 45(25), 8443 (2004).

[44] A. Ulman, An Introduction to Ultrathin Organic Films from Langmuir-Blodgett to Self-Assembly, Academic Press, Boston (1991).

[45] A. Ulman, Chem. Rev. 96, 1533 (1996).

[46] J. Noh, M. Hara, Langmuir 18, 1953 (2002).

[47] C. D. Bain, E. B. Troughton, Y-T. Tao, J. Evall, G. M. Whitesides, and R. G. Nuzzo, J. Am. Chem. Soc. 111, 321 (1989).

[48] S. Park, G. Wang, B. Cho, Y. Kim, S. Song, Y. Ji, M. H. Yoon, T. Lee, Nat. Nanotechnology 7, 438 (2012).

[49] T. W. Kim, G. N. Wang, H. Lee, T. Lee, Nanotechnology 18, 315204 (2007).

[50] J. Taylor, M. Brandbyge, and K. Stokbro, Phys. Rev. Lett. 89, 138301 (2002).

[51] J.L. Vardeman, S.B. Eds, Methods of Experimental Physics Series 28; Academic Press: San-Diego, CA, (1994).

[52] P. J. Rousseeuw, A. M. Leroy, Robust Regression and Outlier Detection; Wiley Series in Probability and Mathematical Statistics; Wiley and Sons: New York, (1987).

[53] H. Yoo, J. Choi, G. Wang, T. W. Kim, J. Noh, T. Lee, Journal of Nanoscience and Nanotechnology 9, 12 (2009).

[54] G. Upton, I. Cook, Understanding Statistics. Oxford University Press, 55 (1996).

[55] D. Zwillinger, S. Kokoska, CRC Standard Probability and Statistics Tables and Formulae, CRC Press, 18 (2000).

[56] K. Seo, H. Lee, ACS Nano 3, 2469 (2009).

국문초록

본 연구에서는 다수의 PEDOT:PSS (3,4-ethylenedioxythiophene) 접합 octanemonothiol(C8)과 octanedithiol(DC8) 분자 소자들이 제작되었으며, 이 소자들로부터 측정된 전기적 특성의 결과에 대하여 통계적 분석이 시행되었다. 각각에 상응하는 통계적 분석 방법들로부터 산술평균, 중앙값, 가우스 평균, 산술 표준편차, 조정 MAD(Median Absolute Deviation) 그리고 가우스 표준편차 등의 다양한 통계 값들을 구할 수 있었으며 또한 Log_{10}(전류 밀도(J)) 히스토그램에 대한 가우스 분포 분석 및 그래프 fitting이 시행되었다. 이어서 각각 C8과 DC8소자들을 대표할 수 있는 통계 값들을 구하고, 이로부터 구하여진 전류밀도-전압(J-V) 특성을 연구하였다. 그리고 이러한 연구로부터 C8 소자의 전기 전도도가 DC8의 그것 보다 약 10배 정도 크다는 것을 알 수 있었다. PEDOT과 PSS의 상이한 특성들로부터, 메틸 말단기를 갖는 C8은 PEDOT과 접하게 되고 싸이올 말단기를 갖는 DC8은 PSS와 접하게 될 것임을 짐작해 볼 수 있었다. 최종적으로 C8과 DC8의 PEDOT:PSS 접합면에서의 차이가 각 분자 소자의 전기 전도도 차이를 불러온다는 것이 이 논문의 결론이다.